

A Miniaturized Multi-Beam Wideband High Gain-5G Antenna Based on a Novel Design of Compact 4x4 Butler Matrix

Mohammed Sadiq¹, Nasri Bin Sulaiman², Maryam BT Mohd Isa²,
Mohd Nizar Hamidon^{2,3}, Muntadher Talib¹

¹ Department of Engineering, Universiti Putra Malaysia, Serdang, Selangor 43400, Malaysia

² Department of Electrical and Electronic Engineering, Faculty of Engineering, Universiti Putra Malaysia, Serdang, Selangor 43400, Malaysia

³ Institute of Nanoscience and Nanotechnology, Universiti Putra Malaysia, Serdang, Selangor 43400, Malaysia

Abstract – This research focuses on developing a uniquely miniaturized 4×4 Butler Matrix Network integrated with a 1×4 linear array antenna, generating four beams with exceptional isolation and transmission coefficients. Extensive analyses evaluate the antenna's radiation characteristics, including gain, directivity, and beam-forming capabilities. Innovative design techniques achieve significant Butler matrix miniaturization without compromising performance, resulting in a compact final design measuring 23mm × 20.5mm. The integrated multi-beam antenna array demonstrates favorable outcomes, ensuring impedance matching at 50Ω, high gain, and four beams directed at angles of ±8° and ±33°. These results highlight the design's superiority over traditional counterparts, with gains of up to 11 dB. Detailed radiation patterns for all ports are presented. The paper also provides insights into the manufacturing process, materials used, and challenges faced. The results conclusively confirm the system's compliance with performance criteria, effectively operating within the 28 GHz frequency band.

DOI: 10.18421/TEM131-81

<https://doi.org/10.18421/TEM131-81>

Corresponding author: Mohammed Sadiq,
Department of Engineering, Universiti Putra Malaysia,
Serdang, Selangor 43400, Malaysia


Email: engmohammedalkaabi@gmail.com

Received: 18 October 2023.

Revised: 29 December 2023.

Accepted: 15 January 2024.

Published: 27 February 2024.

 © 2024 Mohammed Sadiq et al; published by UIKTEN. This work is licensed under the Creative Commons Attribution-NonCommercial-NoDerivs 4.0 License.

The article is published with Open Access at <https://www.temjournal.com/>

This research significantly contributes to downsizing antenna systems, facilitating more compact and efficient communication devices in the future.

Keywords – 5G technology, wideband, Butler-matrix, slot antenna array, multi-beam antenna.

1. Introduction

millimeter-waves (mm-waves) have garnered significant attention as a means to enhance the spectrum efficiency of 5G communication systems, enabling wider bandwidths and faster data rates. Additionally, mm-wave communications facilitate the development of smaller-sized devices [1]. Despite the myriad of advantages offered by 5G technologies, they still contend with challenges such as increased congestion and signal overlap, leading to a decline in Quality of Service (QoS) [2]. Moreover, the escalating number of mobile users places 5G networks under greater traffic loads at higher speeds, necessitating extensive research in the field of beamforming networks to address these issues and improve communication quality, even in unfavorable conditions. To ensure optimal cell coverage without interference or path loss reduction, 5G systems are employing multi-beam antennas. Beamforming represents a pivotal component in expanding the coverage area and enhancing connection quality for mm-wave-based systems. It achieves signal concentration in the desired direction, resulting in increased signal power and reduced power consumption. Furthermore, beamforming significantly reduces interference levels. In the design of a passive beamforming network (BFN), the choice of antenna elements and the BFN structure type are crucial considerations [3].

Multi-beam antennas are frequently employed because the direction of beams in a Phased Array Antenna (PAA) system often depends on phase differences between elements [4]. Modern wireless communication systems heavily rely on multi-beam and beam-scanning antennas to achieve their desired outcomes. Multi-beam antenna concepts have found applications in a variety of domains, including WLANs [5], base stations, satellite communications [6], and even automotive radars [7], providing extensive coverage angles. The benefits of beamforming can be summarized in four key points [8]:

- **Multi-beam Antenna:** Functioning as a switched-beam antenna, and is commonly called a phased array antenna. It generates numerous fixed beams in different directions, guided by predetermined weights assigned to each received signal.

- **Beam Steering:** These beams are directed in specific, discrete directions. Among the multiple available beams, one is selected or steered towards the intended user using a switch, ensuring optimal reception strength. Essentially, the intended signaling beam trails the path of the user.

- **Simplicity:** The selection of a particular beam requires only a beamforming network, an RF switch, and control circuitry.

- **Cost-Efficiency:** The down-conversion to baseband only involves one signal, which is subsequently processed there as all the processing takes place in the RF domain. This offers substantial benefit because circuits that have been down-converted make up one of the most expensive parts of modern wireless networks.

Research on Butler Matrix networks and linear array antenna design and manufacturing has significantly increased in the last few years, particularly in the context of the 28 GHz frequency band, driven by advancements in 5G and beyond. The concept of a four-directional switching beamforming antenna system based on a Butler Matrix installed on a two-layer hybrid stack-up substrate was a significant development in 2019. This substrate comprises two distinct layers, each possessing unique electrical and thermal characteristics. However, adopting a two-layer hybrid stack-up substrate introduced increased complexity and cost to the structure, ultimately failing to reduce overall complexity [9]. In the same year, an alternative strategy was pursued to achieve beamforming capabilities with a phased-array system [10]. This approach allows for continuous steering of a beam in any direction. Nevertheless, it requires intricate beamforming circuitry featuring precise phase shifters, variable gain blocks, and switches, inevitably raising the complexity and cost of system

implementation. One year later, the use of a lens antenna as another approach was explored [11]. When multiple feeds activate the lens at various points, it can alter the direction in which electromagnetic waves propagate, resulting in the generation of multiple radiation beams. While reflector-based and lens-based multi-beam antennas are generally suitable for millimeter-wave frequencies, they suffer from substantial dimensions, rendering them unsuitable for sub-6 GHz base station applications. Unfortunately, this approach also encountered challenges related to complexity management. A research study focused on the design of a compact 4×4 Butler Matrix using substrate integrated waveguide technology for 28 GHz 5G applications was employed [12]. The study highlighted the advantages of this technology, particularly its capacity for size reduction and enhanced performance. Departed from the conventional design of the Butler Matrix Network in pursuit of a smaller form factor, the different components of the proposed design such as branch-line coupler, crossover, and Schiffman line phase shifter are designed and optimized to be low loss and wideband [13]. The total size of the BM is 37 mm × 47 mm. The resulting structure for the proposed Butler Matrix still incorporated four directional couplers, two -45° phase shifters, and one crossover, but it remained relatively large, with a total size of 37 mm × 47 mm. Similarly, in [14] the authors employed the SIW (substrate integrated waveguide) technique for a 3x3 multi-beam antenna at 28 GHz, introducing the Butler Matrix through SIW. However, the cost and complexity associated with the SIW technique posed limitations. In the same year, a conventional multi-beam antenna structure was fabricated [15]. In this design, the traditional Butler Matrix is made up of two phase shifters, four hybrid couplers, and two crossovers, potentially introducing unwanted effects such as side lobes and insertion loss. Consequently, modifications and reductions in the Butler Matrix elements were deemed necessary. A year later, proposed modifications to a 4x4 Butler Matrix to reduce side lobes and enhance the gain of each beam [16]. However, this came at the cost of adding more auxiliary elements, increasing the structural complexity. The study presented a small 2D phased array that was created utilizing Broadside Coupled Stripline (BCS) technology for Sub-6GHz 5G applications. The array was built on a 4x4 Butler Matrix and did not require a crossover. The only components of the suggested Butler Matrix were two 45° phase shifters and four 3dB/90° broadside couplers [17]. A miniaturized Butler matrix design method using a folded structure was introduced in study [18].

The Butler matrix was fabricated in multi-layers using low-temperature co-fired ceramics (LTCC) and designed to operate at 28 GHz. By using the proposed folded structure, the length can be reduced more than two times compared to the general one-layer Butler matrix. Low-temperature co-fired ceramics (LTCC) were used to create a multi-layer substrate for the Butler Matrix, which was then used to implement the suggested architecture. To verify the novel structure, a 4x4 Butler Matrix running at 28 GHz was constructed and measured. In work [19], a proposed Butler Matrix design demonstrated size reduction and improved bandwidth by up to 836 MHz compared to the traditional Butler Matrix. Finally, a new Beamforming Network (BFN) realized in BCS was added to feed antenna arrays measuring 1×4 and 2×2 running at 28 GHz [20]. Couplers and phase shifters were the only components of this innovative BFN. The suggested approach functions without any crossovers, in contrast to the traditional Butler Matrix, which requires two crossovers. The advantageous characteristics of tight coupling and low loss associated with the BCS technology enable the design of a compact and wideband BFN. While these studies offer valuable insights into the design and development of Butler Matrix networks integrated with linear array antennas, there remains a pressing need for further research, especially in the realm of miniaturization, particularly within the 28 GHz frequency band. The purpose of this work is to advance this rapidly developing field of study by introducing a unique design that stands as the smallest of its kind. The 28 GHz frequency band has emerged as pivotal in this evolution, owing to its potential for high data rates [21]. However, fully harnessing this potential necessitates the creation of efficient and compact antenna systems. Because of their ability to produce beamforming, the pairing of a Butler Matrix network with linear array antennas has attracted a lot of interest, holding the promise of significantly improving the performance of wireless communication systems [22]. The integration of these two components offers the prospect of an advanced antenna system that amalgamates the beamforming prowess of a Butler Matrix with the high gain and directivity inherent to a linear array antenna. Nevertheless, the design and fabrication of a 4x4 Butler Matrix network seamlessly integrated with a 1×4 linear array antenna, tailor-made for the 28 GHz frequency band while maintaining an exceptionally compact size, presents a distinctive set of challenges. Existing literature and prior designs often fall short in meeting the stringent size constraints and performance criteria demanded by contemporary wireless communication devices.

The primary objective of this research is to develop an antenna system that strikes a harmonious balance between meeting the stringent performance demands of the 28 GHz spectrum and adhering to the size constraints imposed by contemporary devices. Our innovative design brings together the exceptional beamforming capabilities of the Butler Matrix network and the 1×4 linear array antenna to elevate the overall performance and spatial diversity of the system. In our approach, we introduce a modified conventional BM for 5G systems by eliminating one of the crossover elements, resulting in the formation of four orthogonal beams. These beams are directed in different directions, effectively reducing interference from nearby users and expanding coverage. The 1×4 slotted antenna array is first simulated and then integrated onto a single-layer planar substrate with a BM circuit designed. This integration leads to multi-beam radiation, which is rigorously simulated using the Ansoft HFSS simulator. This paper provides comprehensive insights into our design strategies, the unique manufacturing process, and the stringent testing methods employed to validate this pioneering system. Successful completion of this research will contribute significantly to the ongoing efforts aimed at developing compact and efficient antenna systems. The following sections are arranged as such: research contributions in Section 2, 5G-BM design in Section 3, 5G antenna array design in Section 4, simulation outcomes in Section 5, and the conclusion in Section 6.

2. Contribution

This paper presents an innovative and unique approach to the design and manufacture of a 4x4 Butler Matrix network integrated with a 1×4 linear array antenna operating in the 28 GHz frequency band. Its distinct contribution to the field can be identified in the aspect of miniaturization. This research contributes to the ongoing efforts in miniaturizing Butler Matrix networks without compromising their performance. The proposed design is the smallest of its kind, representing a significant leap in the development of compact antenna systems suitable for modern wireless communication devices. The design methodology integrating a 4x4 Butler Matrix with a 1×4 linear array antenna, tailored specifically for the 28 GHz frequency band, is a novel contribution. The unique design exploits the advantages of both systems, offering enhanced beamforming capabilities, high gain, and better directivity.

In summary, the study fills a vital void in the literature, making a substantial addition to the wireless communication domain, providing a practical solution to real-world challenges, and offering valuable insights for future research.

3. 5G-BM Structure Design

A typical scheme proposed for a 4-beam BM contains hybrid branch-line couplers, one crossover, and two-phase shifters, built in and optimized using Keysight ADS software. BM elements consist of transmission lines. Microstrip feed line equations are used to calculate element lengths. It is created by perfect conductor (copper) strips printed on a Roger-RO4003 substrate layer (at 0.305 mm thickness, 3.55 dielectric constant, and 0.0022 loss tangent) which isolate the BM elements from the ground plane. Figure 1 illustrates the phase difference between P3 and P4. The Hybrid Branch Line Coupler (HPLC) is built using microstrip line connectors, input ports, and power probe to measure the output power. In addition, simulators such as Large Signal Scattering Parameter (LSSP) and Harmonic Balance (HB) are employed for the evaluation of the reflection coefficient.

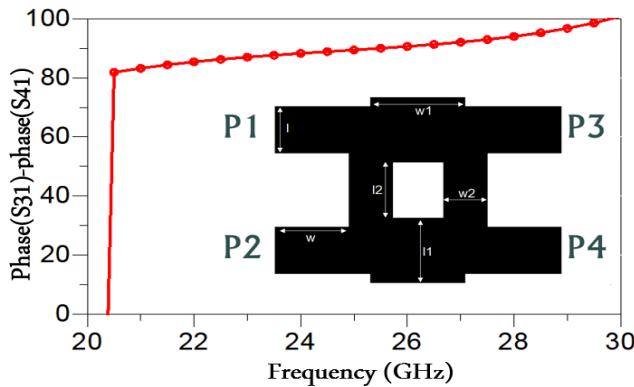


Figure 1. The HPLC simulated results for the phase difference of HPLC output ports and HPLC structure ($l=0.936$, $w=1.28$, $l_1=0.876$, $w_1=1.29$, $l_2=1.09$, $w_2=0.758$) mm

The HPLC simulated results of S parameters are shown in Figure 2, presented in the layout window in ADS. Based on $((N/2) \times \log_2 N)$, the sum of HPLC used in the $(N \times N)$ BFN configuration is determined [3]. Two pairs of $Z_0 \Omega$ and $(Z_0 / \sqrt{2}) \Omega, \lambda_c / 4$ microstrip lines, whereby Z_0 denotes the feed line impedance, are used to realize HPLC [9]. The phase difference between P3 and P4 is displayed in Figure 2(a), whereby the reflection coefficient (S13) and (S14) are approximately -3 dB -5 dB at resonance frequency (28GHz). In addition, Figure 2(b) plots the simulated S parameters, showing the HPLC parameters' optimized design.

The reflection coefficient (S11) and isolation (S212) below -22 dB is attained across a broad frequency range (20GHz – 30GHz) [23].

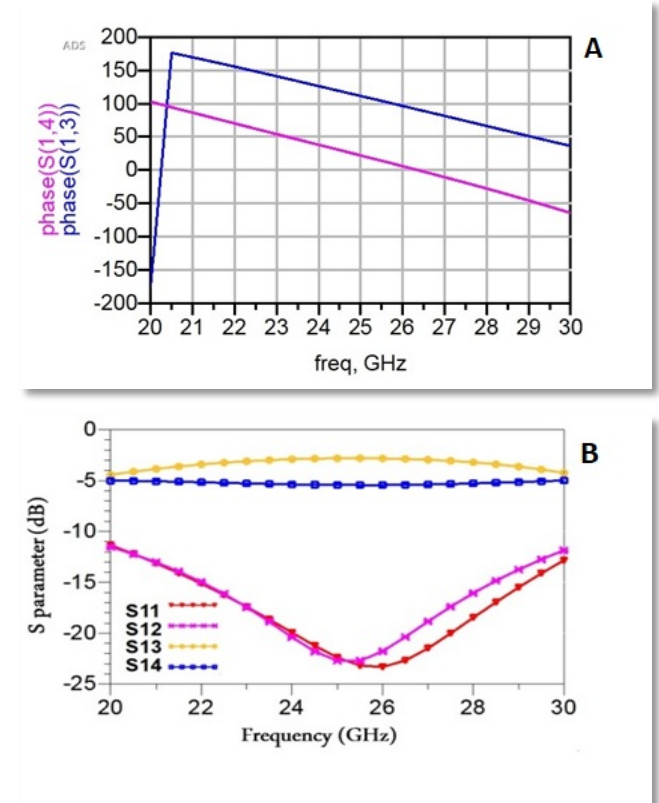


Figure 2. The HPLC simulated results (a) phase difference of the (b) S-parameters of the circuit

The simulated phase difference is, on average, within $\pm 5^\circ$ of the theoretical 90° phase difference over the frequency range of (20-30) GHz. As such, the HPLC scattering matrix is as follows:

Even mode:

$$\begin{bmatrix} K & L \\ M & N \end{bmatrix} = \begin{bmatrix} 1 & 0 \\ jY_L & 1 \end{bmatrix} \begin{bmatrix} 0 & jZ_K \\ jY_K & 0 \end{bmatrix} \begin{bmatrix} 1 & 0 \\ jY_L & 1 \end{bmatrix} \quad (1)$$

$$\Gamma_e(S11) = \frac{K+L-M-N}{K+L+M+N} = 0 \quad (2)$$

$$R_e(S21) = \frac{2}{K+L+M+N} = -\frac{(1+j)}{\sqrt{2}} \quad (3)$$

Odd mode:

$$\begin{bmatrix} K & L \\ M & N \end{bmatrix} = \begin{bmatrix} 1 & 0 \\ -jY_L & 1 \end{bmatrix} \begin{bmatrix} 0 & jZ_K \\ jY_K & 0 \end{bmatrix} \begin{bmatrix} 1 & 0 \\ -jY_L & 1 \end{bmatrix} \quad (4)$$

$$\Gamma_o(S11) = \frac{K+L-M-N}{K+L+M+N} = 0 \quad (5)$$

$$R_o(S21) = \frac{2}{K+L+M+N} = -\frac{(1-j)}{\sqrt{2}} \quad (6)$$

Having characteristic admittance of the conventional branch-line coupler $Y_K = \frac{1}{Z_K}$ and $Y_L = \frac{1}{Z_L}$, where R_e , Γ_e and R_o , Γ_o respectively denote the even and odd modes' transmission and reflection coefficients.

Consequently, to ensure optimal matching conditions, the conventional BLC's scattering parameter matrix can be denoted as:

$$[S] = \begin{bmatrix} S_{11} & S_{12} & S_{13} & S_{14} \\ S_{21} & S_{22} & S_{23} & S_{24} \\ S_{31} & S_{32} & S_{33} & S_{34} \\ S_{41} & S_{42} & S_{43} & S_{44} \end{bmatrix} = \frac{1}{\sqrt{2}} \begin{bmatrix} 0 & j & 1 & 0 \\ j & 0 & 0 & 1 \\ 1 & 0 & 0 & j \\ 0 & 1 & j & 0 \end{bmatrix} \quad (7)$$

Two HBLCs can be combined to make a crossover. The crossover's configuration is shown in Figure 3. The signals are passed to the second stage via the crossover with a 0dB insertion loss and no other losses. The crossover scattering matrix is provided as follows [24]:

$$[S] = \begin{bmatrix} 0 & 0 & j & 0 \\ 0 & 0 & 0 & j \\ j & 0 & 0 & 0 \\ 0 & j & 0 & 0 \end{bmatrix} \quad (8)$$

With regards to the section on the conventional transmission line, the KLMN matrix is given by:

$$\begin{bmatrix} K & L \\ M & N \end{bmatrix}_{\lambda/4} = \begin{bmatrix} \cos \theta & jz \sin \theta \\ j & \cos \theta \end{bmatrix} \begin{bmatrix} 0 & jZ_0 \\ j & 0 \end{bmatrix} \quad (9)$$

Finally, the scattering parameters are given as:

$$S_{11} = \frac{s_{11}^e + s_{11}^o}{2} \quad (10)$$

$$S_{21} = \frac{s_{21}^e + s_{21}^o}{2} \quad (11)$$

$$S_{31} = \frac{s_{31}^e + s_{31}^o}{2} \quad (12)$$

$$S_{41} = \frac{s_{41}^e + s_{41}^o}{2} \quad (13)$$

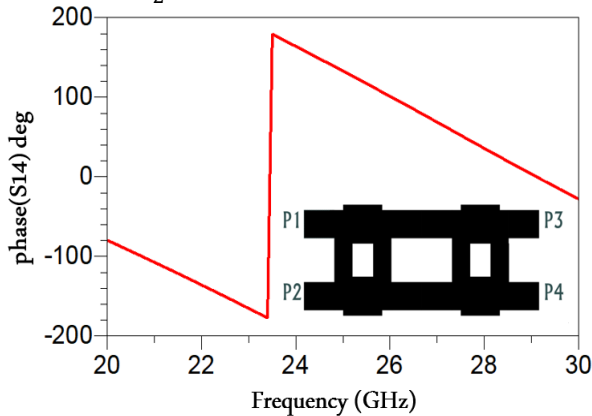


Figure 3. The crossover simulated results (a) the S-parameters (b) the phase difference of crossover output ports and crossover structure

Figure 4(a) presents the phase difference of the crossover output ports. As observed in Figure 4(b), the simulated S-parameters and the insertion loss S14 are approximately -3.9 across a wide frequency range (20-30) GHz.

In addition, S11, S12, and S13 are less than -17 GHz at the operating frequency. Furthermore, the phase shifter is designed.

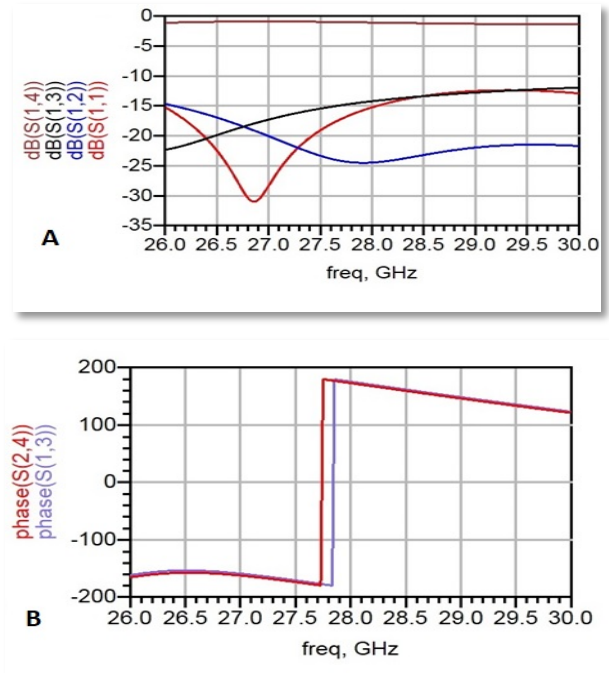


Figure 4. The crossover simulated results (a) phase difference of crossover output ports (b) the S-parameters

Figure 5 presents the schematic structure configuration of a designed phase shifter. We conducted a thorough analysis of the phase shifter's functionality, with specific emphasis on its performance at a frequency of 28 GHz. Our experimental results demonstrate a significant alignment with the theoretical expectations, notably in terms of the phase shift value.

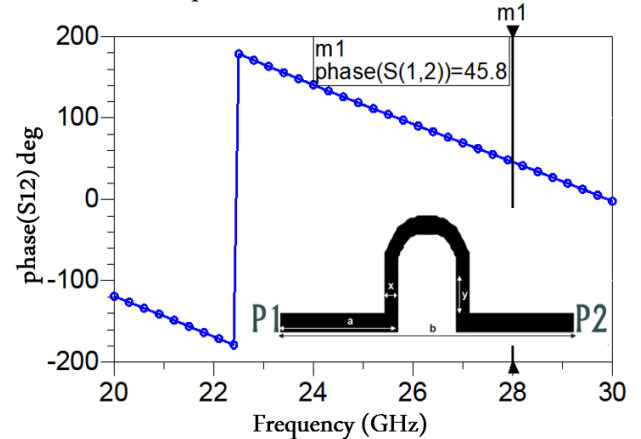


Figure 5. The phase difference of the phase shifter with its schematic ($a=3.08$ $b=8.71$ $x=0.4$ $y=1.2$) mm

Indeed, the phase shifter's indicator was found to be approximately equal to the theoretical value of 45 degrees, as shown in Figure 6. This outcome strongly supports the precision of our theoretical model and underscores the effectiveness of the phase shifter at the specified frequency.

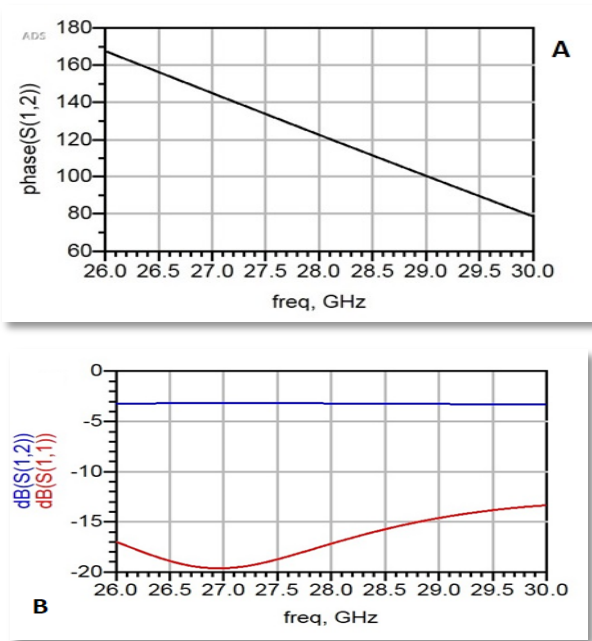


Figure 6. The phase shifter simulation result (a), the phase difference (b) the S-parameters

As depicted in Figure 7, the layout design is evident. Ports 1 through 4 serve as the input ports, while ports 5 through 8 are connected to the antenna network, serving as the output ports. The intended purpose of this BM is to uniformly supply all elements in the antenna array with equal amplitudes and equally varying phase shifts. By exciting different input ports, theoretically, various phase shifts can be achieved $[-135^\circ, -45^\circ, 45^\circ, \text{ and } 135^\circ]$ [3]. Consequently, it is possible to steer the beam in various directions. The overall size measures $15\text{mm} \times 17\text{mm}$, approximately equivalent to $(1.4 \times 1.58) \lambda_c^2$, where λ_c represents the wavelength at 28 GHz.

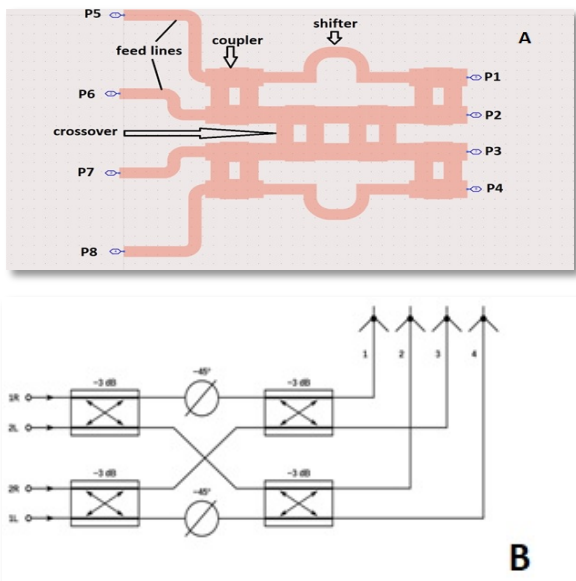


Figure 7. The layout design (a) 4×4 Butler Matrix proposed (b) Butler Matrix construction

The insertion and isolation coefficients for each port have been analyzed, as indicated in Figure 8. Due to the BM's symmetric nature, the excitation results of P1 are similar to those of P4, and P2 is similar to P3. In Figure 8, when the input ports (P1, P2) are excited, the simulated S parameters of the suggested BM are displayed. It is important to note that a 50Ω load is used as a terminator as one out of the four input ports is excited, and the rest are terminated. When the first port is excited, as depicted in Figure 8(a), the coupling and reflection coefficients remain consistently below -15 dB over a wide (26-30) GHz frequency range. While running at 28 GHz, the following depict the simulated insertion losses from P1 to the P5-P8 output ports: -6.943 dB, -8.236 dB, -6.943 dB, and -8.475 dB, accordingly. Likewise, as P2 is excited (Figure 8(b)), the levels of coupling and reflection across the frequency range of 26-30 GHz remain above -15 dB. At 28 GHz, the simulated insertion losses from P2 to P5-P8 are as follows: -8.498 dB, -8.799 dB, -6.579 dB, and -9.019 dB, respectively.

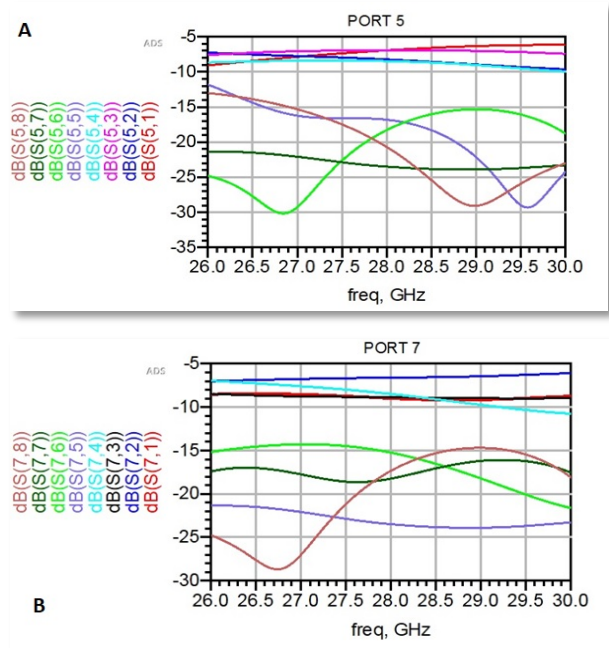


Figure 8. The insertion and reflection loss for the proposed BM when excited (a) input ports (1 or 4) (2 or 3) (b) output ports (5 or 8) (6 or 7)

Figure 9 shows the extent to which the surface current distribution is produced on the 4×4 BM at 28 GHz, which is stimulated by the HFSS simulator, where we notice the intense density of the current distribution at the exciting input port and its decline at the other input ports. At the same time, all the output ports have a strong current density, similar to when exciting other input ports.

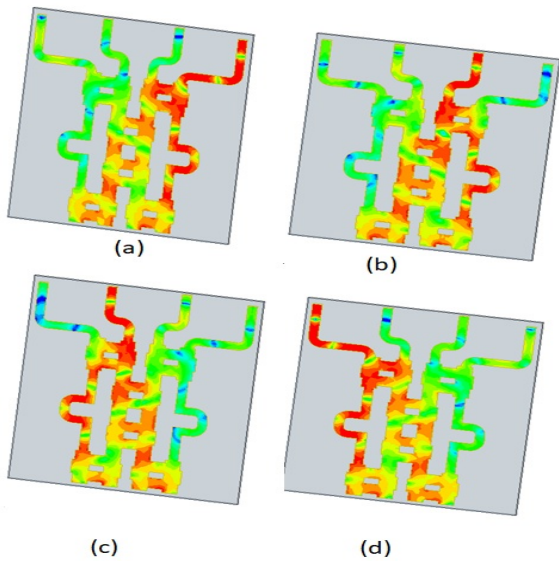


Figure 9. The current distributions for the proposed BM when excited (a) Port-1 (b) Port-2 (c) Port-3 (d) Port-4

4. 5G Antenna Array Design

The proposed BFN is connected to a simple patch array antenna running at 28 GHz, with four rectangular slotted patch antennas at 5mm×18.5mm. Figure 10 shows the proposed design, with the dimensional parameters indicated in the caption. It employs the inverted U slot which could resonate easily at the operating frequency without mutual coupling [25], [26]. A uniform linear array is adopted to physically match the modified BM proposed. The Roger-RO4003 is the dielectric material utilized for the substrate, with a 0.305 mm thickness. With regards to antenna feeding, a multi-microstrip feed is employed due to its appropriateness for a direct merger with the BM.

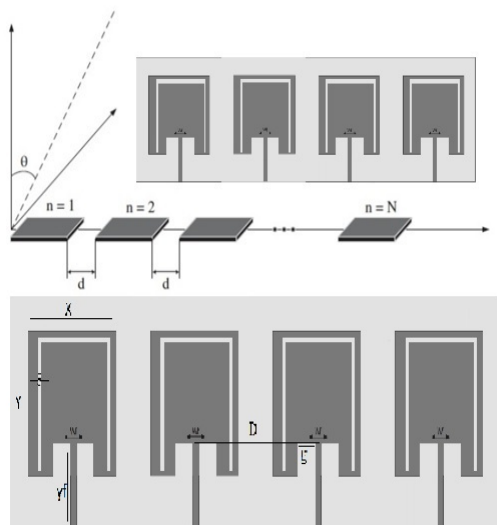


Figure 10. The schematic of the proposed 5G antenna array, with the following dimensions ($X = 2.5$, $Y = 2.83$, $xf = 0.4$, $yf = 1.5$, $D = 4.5$, $g = 0.35$, $s = 0.1$) mm

Figure 11(a) presents the antenna’s simulation outcomes, showing the reflection loss for all the ports from p1 to p4 namely -29, -17.5, -17.2, and -27.5 dB, respectively. The mutual coupling readings are demonstrated as follows $S_{21} = -12.1$ dB, $S_{32} = -10.2$ dB, and $S_{43} = -12$ dB. The 3D graphical gains are displayed in Figure 11(b) with a high gain of 9 dB. This indicates a high-performance antenna that can be combined with a butler to obtain multiple high-efficiency beams. Figure 11(c) displays the antenna gain which also indicates a high-performance antenna that can be combined with a butler to obtain multiple high-efficiency beams.

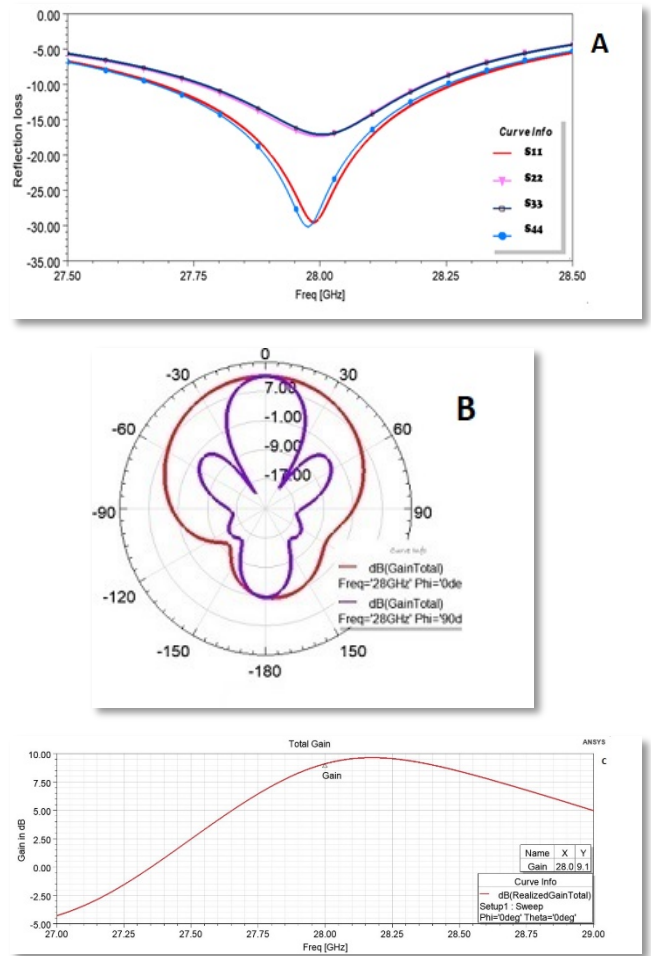


Figure 11. The antenna array simulated results: (a) the S-parameters, (b) 2D polar sketch for E and H plane, and (c) the total gain

Figure 12 shows the radiation patterns in the xz-plane and yz-plane, whereby the antenna array is shown to have a directional radiation pattern and high gain. Accordingly, all the simulation results give a good indicator for merging with the proposed Butler Matrix.

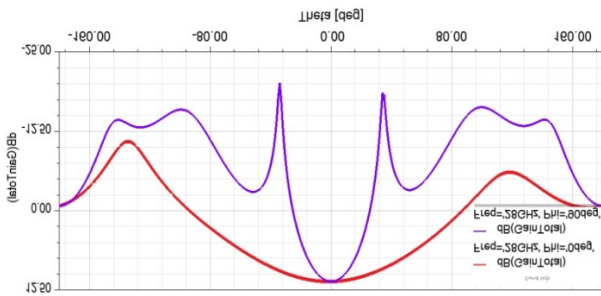


Figure 12. The radiation pattern in two plane xz-plane

The proposed antenna has been compared with several antennas in related works. The results are summarized in Table 1. Unlike most of the reported antennas, the proposed antenna does not demonstrate a higher gain. However, a gain is achieved when it is combined with the BMN. Moreover, it is much smaller than the conventional antenna while keeping a directional radiation pattern.

Table 1. Differences between the single beam antenna array and other designs

Ref. (year)	Freq (GHz)	Gain (dB)	Seize (mm ²)	Polari zation	Microstrip Type
[27] (2018)	2-3.1	2.73	35×5	LP	Single slot
[28] (2019)	1.8-2.5	11	200×200	dual polari ze	2×2 square
[29] (2019)	multi -band	10.56	30 × 25	CP	4×2 square
[30] (2019)	10.4	9.8	27 × 27	C	2×2 square
[31] (2020)	1.7-2.9	9- 4.5	56 × 75.5	CP	single square loop
[32] (2020)	0.91-2.55	5-8.3	165 × 165	LP	2×2 fractal
[33] (2021)	27-45	14.8-14.1	16.5 × 16.5	Dual-Linear	2×2
[34] (2022)	37	12.8	20 × 40	LP	1×4 single feed
Proposed	28	9	5×18.5	CP	1×4square

5. Simulation and Fabrication Results

Finally, to demonstrate the multi-beam performance of the above components, direct incorporation between a slotted array antenna with a proposed BM is investigated. All the realized components have been arranged on the same layer and printed on the Roger-RO4003. As illustrated in Figure 13, the schematic of the final design with all dimensions has a total size of 23mm × 20.5mm. Each BM's output port serves as a feeding line for the antenna array elements connected to them.

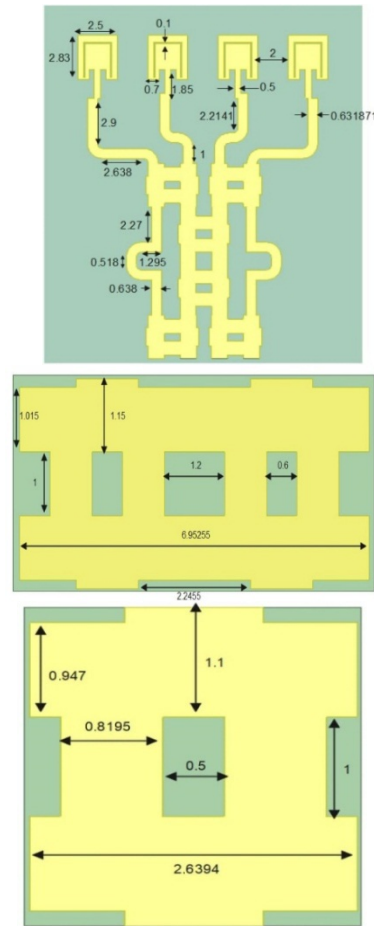


Figure 13. The schematic of the 5G multi-beam antenna proposed

Figure 14 shows that the reflection and mutual coefficients are less than -11dB over the operating frequency of all the input ports. Four beams with different directions are acquired. A certain proportion of power is assigned to an input port, delivered over the network, and a constant phase difference is produced between the neighboring output ports. Based on that, the direction of the antenna beams under each port input phase is different. Then after integrating and completing the multi-beam antenna array simulation, it achieved matching at 50Ω and high gain with four beams directed at an angle of ±8° and ± 33° beams.

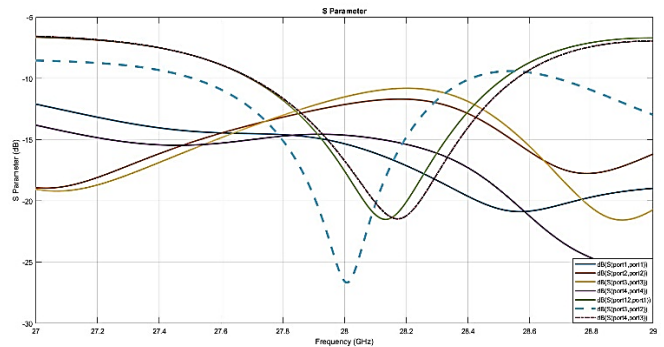


Figure 14. The S parameter of the multi-beam antenna proposed

Figure 15 displays photographs of the proposed design and the result after manufacturing. To conduct the test, we activated only one port and studied it individually. This approach is necessary due to the significant size difference between the SMA connector and the antenna.

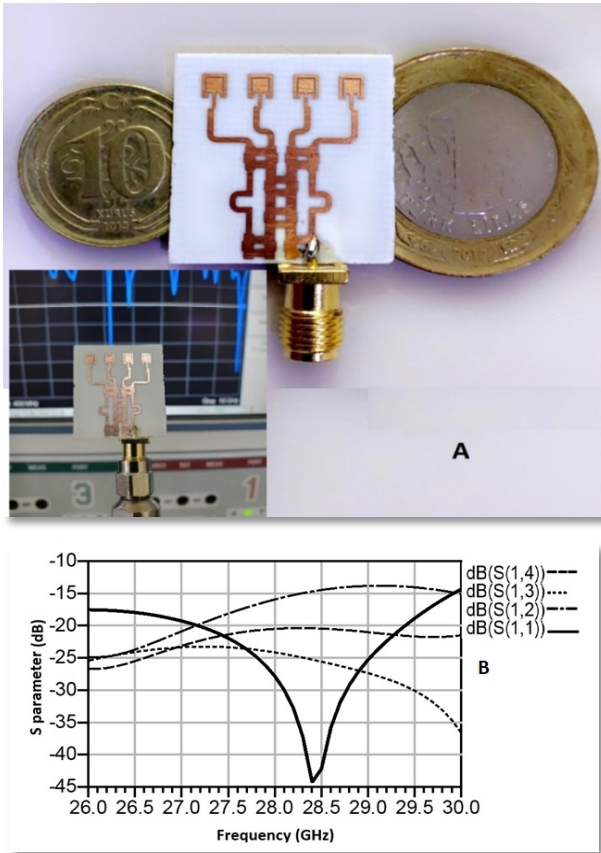


Figure 15. BFN antenna array (a) Photograph of the BFN antenna array under test, (b) Measured S-Parameter results of the BFN antenna array

The antenna array's measured and simulated findings demonstrate the wideband, which uses a comparatively large range of frequencies. Figure 16 shows the simulation results for a polar radiation pattern, whereby a high gain with a high directive beam can be obtained.

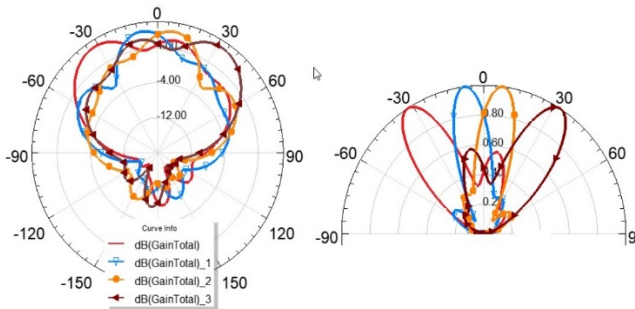


Figure 16. The 2D radiation pattern driven by the proposed multi-beam antenna (the gain for the 4 beams and normalized gain)

By presenting the previous results and comparing the differences between Figure 16 and Figure 11, the following results are obtained:

- 1- A multi-beam is obtained instead of one beam.
- 2- The side lobe is close to fading or almost ineffective.

The distinction in beam angles becomes apparent when the BMN is integrated with the antenna array, as seen in the preceding figure, and when the BMN operates independently without an antenna, as illustrated in Figure 17.

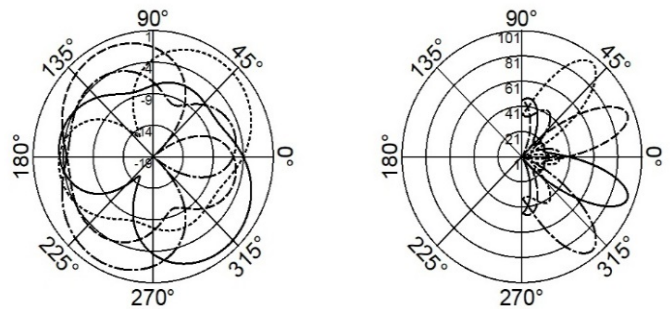


Figure 17. Radiation pattern polar plot against output power (mW)

Table 2 shows the primary direction when port1, port2, port3, and port4 are excited for the Butler Matrix without antenna.

Table 2. The progressive phase variation and scanning beam angle across output ports for BM

Output Port no.	Progressive phase (ph)	Scan beam angle (angle)
Port5	-48°	-20°
Port6	-115°	-52°
Port7	115°	52°
Port8	48°	20°

Figure 18 shows the difference in gain for the antenna without Butler Matrix (Figure 18a) and antenna with Butler Matrix (Figure 18b). The improvement can be seen in the gain that describes the capability of the antenna in converting radio waves received from a specific direction into electric energy, so the system performance will be high. The gain comparison between the antenna without Butler Matrix and antenna with Butler Matrix is shown in Table 3.

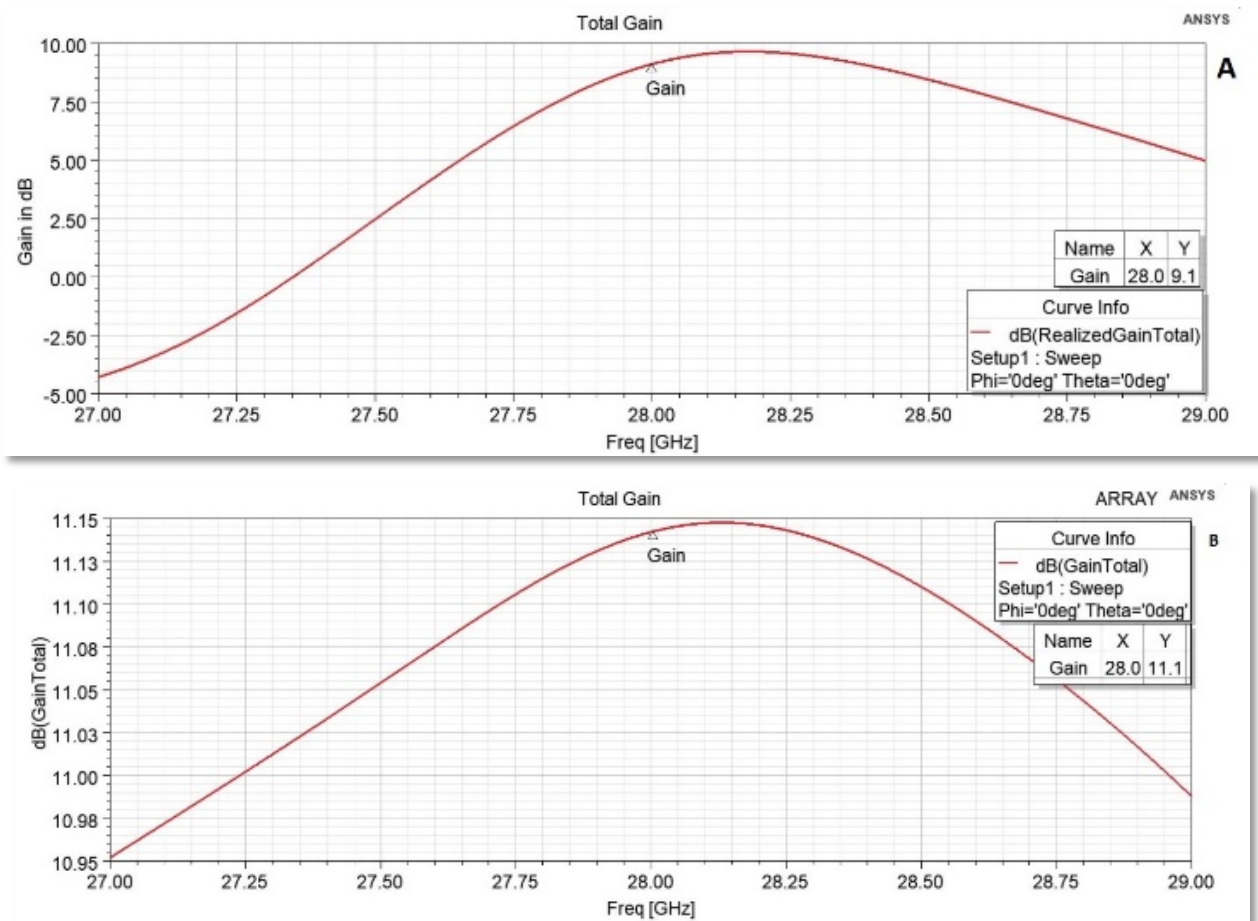


Figure 18. The realized gain for the (a) antenna without Butler Matrix and (b) antenna with Butler Matrix

Table 3. The gain comparison between antenna without Butler Matrix and antenna with Butler Matrix

Gain in dB without Butler Matrix	9
Gain in dB with Butler Matrix	11

With regards to the Butler Matrix network, there is potential to conserve power from being lost to no avail and use it only when needed, as shown in Figure 9. If any of the four ports is turned on, it gives the same results as shown in Figure 19; if more than one port is turned on, the difference is indicated by the increase in power.

Figure 19(a) presents the gain when one port is activated, whilst Figure 19(b) demonstrates the gain when two ports are activated. Figures 19(c) and 19(d) present the gain value when three and four ports are activated, respectively, whereby the gain is at its highest value of 11 dB as shown in Table 4.

Table 4. The realized gain for four cases

Ports count	1	2	3	4
Gain in dB	4.4	6.63	9	11

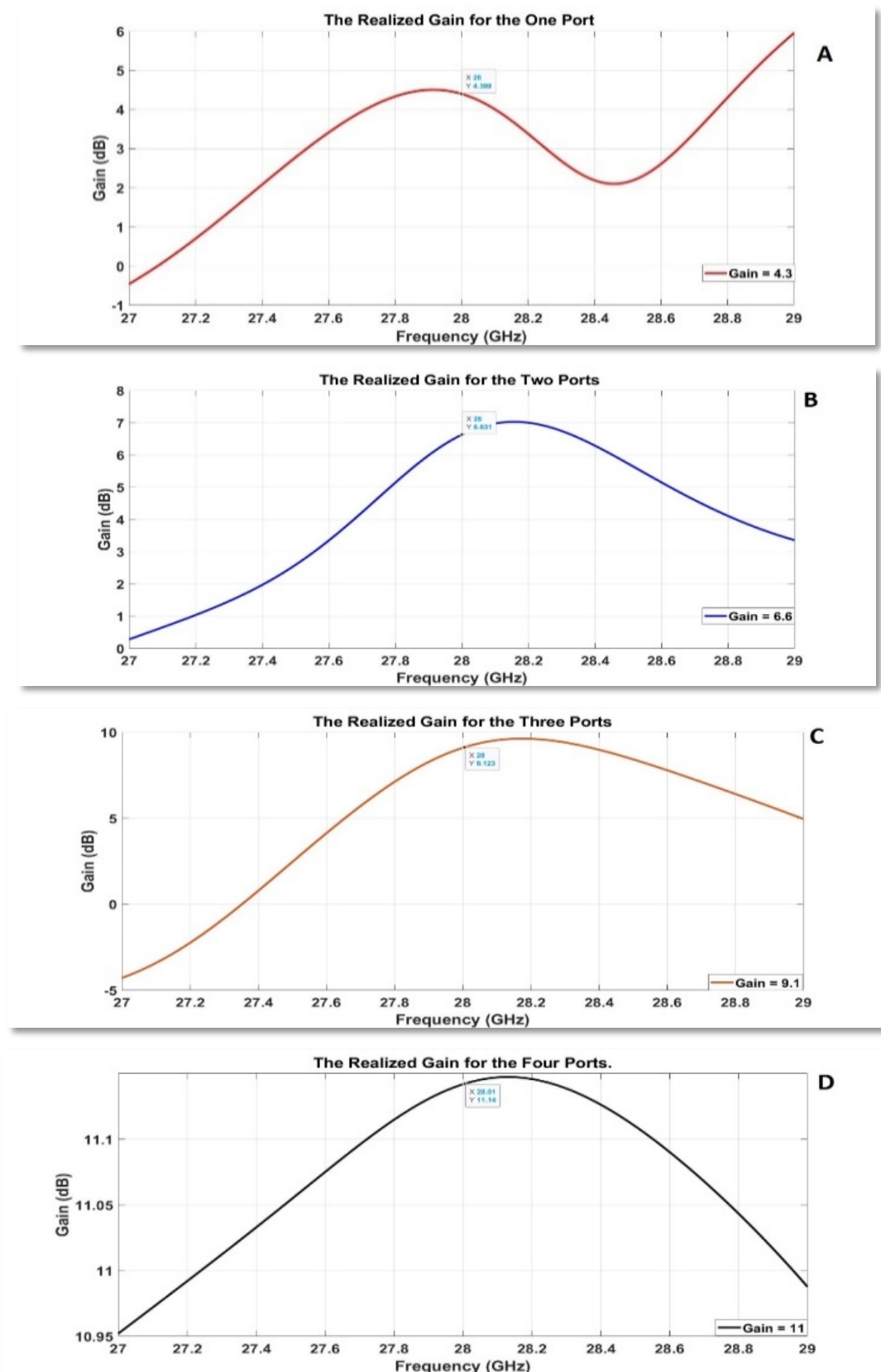


Figure 19. The realized gain for the activation of (a) one port, (b) two ports, (c) three ports, and (d) four ports

Table 5 presents a summary of and comparison between the current study and past research. This current study concentrates on the complete integration of the antenna elements and Butler Matrix operating at 28 GHz.

Past studies [35], [36], [37] which showed comparable operating frequencies were selected to be compared. [38] Operated at a frequency of 30 GHz instead of 28 GHz.

Nonetheless, studies [35], [36], [37], [38] are still compared due to their microstrip line structure, similar to that of the current study. An off-the-shelf, commercially-available packed switch chip was used in [37]. As it does not have an in-built switch, it saves cost and simplifies the manufacturing process. When comparing this work with the others, we found that it achieves an excellent balance between size and gain, which is the opposite of what we found in [36] and [38] which achieved gain improvement at the expense of size. Meanwhile, [35] and [37] did not achieve an acceptable gain or a small size. With simplicity of design, we are able to offer the smallest, inexpensive, and easy to fabricate design, which in turn offers many facilities in integration with other devices.

Table 5. Differences between the suggested BM design and other designs

Ref. Year	Freq GHz	BM	Switch	count Beam Direction	Gain [dB]	Dimension mm ²
[35] 2019	28	4 × 4 Micro strip	No Switch	4	5.2	36.2 × 44.3
[36] 2019	28	4 × 4 Micro strip	No Switch	4	12	95 × 32
[37] 2021	28	4 × 4 Micro strip	Absorptive SP4T Commercial Silicon	4	4.5	36 × 48
[38] 2021	30	4 × 4 Micro strip	No Switch	4	9	50 × 52
Proposed	28	4 × 4 Micro strip	No Switch	4	11	20 × 20.5

6. Conclusion

This research focuses on the development and fabrication of a uniquely miniaturized 4×4 Butler Matrix network combined with a 1×4 linear array antenna, leading to the creation of four beams with excellent isolation and transmission coefficients. The study commences by outlining the Butler Matrix network and array antenna's theoretical framework, delving into critical design aspects like phase shifters, crossovers, hybrid couplers, and feed networks. Extensive analyses are conducted to assess the antenna's radiation characteristics, encompassing gain, directivity, and beam-forming capabilities.

The miniaturization of the Butler Matrix is achieved through innovative design techniques, leading to a substantial reduction in size without compromising performance. Following the integration and completion of the multi-beam antenna array simulation, favorable outcomes are achieved, including impedance matching at 50Ω and high gain, with four beams oriented at angles of ±8° and ±33°. These results underscore the superiority of the proposed design over its traditional counterparts, with gains reaching up to 11 dB. Notably, the compact final design measures at 23mm × 20.5mm, making it easily integrable with other devices. The results conclusively demonstrate that the proposed system meets the expected performance criteria and effectively operates within the targeted 28 GHz frequency band. This research significantly contributes to the ongoing efforts to downsize antenna systems, paving the way for more compact and efficient communication devices in the future.

References:

- [1]. Seker, C., Güneser, M. T., & Ozturk, T. (2018). A review of millimeter wave communication for 5G. In *2018 2nd International Symposium on Multidisciplinary Studies and Innovative Technologies (ISMSIT)*, 1-5. Ieee.
- [2]. Salahdine, F., Han, T., & Zhang, N. (2023). 5G, 6G, and Beyond: Recent advances and future challenges. *Annals of Telecommunications*, 1-25.
- [3]. Babale, S. A., Rahim, S. K. A., Barro, O. A., Himdi, M., & Khalily, M. (2018). Single Layered 4×4 Butler Matrix Without Phase-Shifters and Crossovers. *IEEE Access*, 6, 77289-77298.
- [4]. Vallappil, A. K., Rahim, M. K. A., Khawaja, B. A., Murad, N. A., & Mustapha, M. G. (2020). Butler matrix based beamforming networks for phased array antenna systems: A comprehensive review and future directions for 5G applications. *IEEE Access*, 9, 3970-3987.
- [5]. Matsuo, S., Miyamoto, S., Nakajo, H., & Fujii, T. (2023). Beam Pattern Estimation of 5G Millimeter-Wave Base Station Based on Radio Map and Multi-Beam Antenna Model at 28GHz. In *2023 International Conference on Information Networking (ICOIN)*, 7-12. IEEE.
- [6]. Liu, X., Yan, Z., Wang, E., Zhao, X., Zhang, T., & Fan, F. (2023). Multibeam Forming With Arbitrary Radiation Power Ratios Based on a Conformal Amplitude-Phase-Controlled Metasurface. *IEEE Transactions on Antennas and Propagation*, 71(4), 3707-3712.
- [7]. Han, K., Li, W., & Liu, Y. (2019). Flexible phase difference of 4× 4 Butler matrix without phase-shifters and crossovers. *International Journal of Antennas and Propagation*, 2019, 1-7.
- [8]. Sadiq, M., bin Sulaiman, N., Isa, M. M., & Hamidon, M. N. (2022). A Review on Machine Learning in Smart Antenna: Methods and Techniques. *TEM Journal*, 11(2), 695.

- [9]. Kim, S., Yoon, S., Lee, Y., & Shin, H. (2019). A miniaturized Butler matrix based switched beamforming antenna system in a two-layer hybrid stackup substrate for 5G applications. *Electronics*, 8(11), 1232.
- [10]. Ojaroudi Parchin, N., Alibakhshikenari, M., Jahanbakhsh Basherlou, H., Abd-Alhameed, R., Rodriguez, J., & Limiti, E. (2019). MM-wave phased array quasi-yagi antenna for the upcoming 5G cellular communications. *Applied Sciences*, 9(5), 978.
- [11]. Campo, M. A., Carluccio, G., Blanco, D., Litschke, O., Bruni, S., & Llombart, N. (2020). Wideband circularly polarized antenna with in-lens polarizer for high-speed communications. *IEEE Transactions on Antennas and Propagation*, 69(1), 43-54.
- [12]. Lu, R., Yu, C., Zhu, Y., & Hong, W. (2020). Compact millimeter-wave endfire dual-polarized antenna array for low-cost multibeam applications. *IEEE Antennas and Wireless Propagation Letters*, 19(12), 2526-2530.
- [13]. Imani, A., & Bayati, M. S. (2021). A novel design of compact broadband 4×4 Butler matrix-based beamforming antenna array for C-Band applications. *AEU-International Journal of Electronics and Communications*, 138, 153901.
- [14]. Md Jizat, N., Yusoff, Z., A/L Nallasamy, A., & Yamada, Y. (2021). 5G Millimeter-Wave Beamforming System using Substrate Integrated Waveguide. *F1000Research*, 10, 1311.
- [15]. Jeon, M., Seo, Y., Cho, J., Lee, C., Jang, J., Lee, Y., ... & Kahng, S. (2021). Investigation on beam alignment of a microstrip-line Butler matrix and an SIW Butler matrix for 5G beamforming antennas through RF-to-RF wireless sensing and 64-QAM tests. *Sensors*, 21(20), 6830.
- [16]. Alsirhani, A., Ezz, M., & Mostafa, A. M. (2022). Advanced Authentication Mechanisms for Identity and Access Management in Cloud Computing. *Computer Systems Science & Engineering*, 43(3).
- [17]. Temga, J., Shiba, T., & Suematsu, N. (2022). A Compact 2-D Phased Array Fed by 4×4 Butler Matrix Without Crossover in Broadside Coupled Stripline For Sub-6GHz 5G Applications. In *2022 52nd European Microwave Conference (EuMC)*, 540-543. IEEE.
- [18]. Nam, S., Choi, S., Ryu, J., & Lee, J. (2022). Compact 28 GHz folded Butler matrix using low-temperature co-fired ceramics. *Journal of Electromagnetic Engineering and Science*, 22(4), 452-458.
- [19]. Abdulbari, A. A., Rahim, S. K. A., Tan, K. I. M., Hanoosh, H. O., & Jawad, M. M. (2023). Compact 4×4 Butler matrix design-based switch beamforming antenna array for 5G applications. *Authorea Preprints*.
- [20]. Temga, J., Edamatsu, K., Furuichi, T., Motoyoshi, M., Shiba, T., & Suematsu, N. (2023). 1-D and 2-D Beam Steering Arrays Antennas Fed by A Compact Beamforming Network for Millimeter-Wave Communication. *IEICE Transactions on Communications*, 2022EBP3113.
- [21]. Li, M., Zhang, F., Ji, Y., & Fan, W. (2022). Virtual antenna array with directional antennas for millimeter-wave channel characterization. *IEEE Transactions on Antennas and Propagation*, 70(8), 6992-7003.
- [22]. Shallah, A. B., Zubir, F., Rahim, M. K. A., Majid, H. A., Sheikh, U. U., Murad, N. A., & Yusoff, Z. (2022). Recent developments of butler matrix from components design evolution to system integration for 5g beamforming applications: A survey. *IEEE Access*, 10, 88434-88456.
- [23]. Pozar, D. M. (2011). *Microwave engineering*. John wiley & sons.
- [24]. Heba, E. H., & FATTOUM, M. K. (2022). Dual Band Branch-Line Coupler Using Stub-Loaded Lines. *The Eurasia Proceedings of Science Technology Engineering and Mathematics*, 21, 430-434.
- [25]. Sadiq, M., Sulaiman, N. B., Mohd, M. B., & Hamidon, M. N. (2022). Design and Simulation of Meander Line Antenna for Operating Frequency at 2.5 GHz Based on Defected Ground Structure. In *Next Generation of Internet of Things: Proceedings of ICNGIoT 2022*. Singapore: Springer Nature Singapore.
- [26]. Sadiq, M., Sulaiman, N. B., Mohd, M. B., & Hamidon, M. N. (2022). Multiband Handheld Antenna with E-shaped Monopole Feeding. In *Next Generation of Internet of Things: Proceedings of ICNGIoT 2022*, 391-398. Singapore: Springer Nature Singapore.
- [27]. Shi, Y., Fan, Y., Li, Y., Yang, L., & Wang, M. (2018). An efficient broadband slotted rectenna for wireless power transfer at LTE band. *IEEE transactions on Antennas and Propagation*, 67(2), 814-822.
- [28]. Shen, S., Zhang, Y., Chiu, C. Y., & Murch, R. (2019). A triple-band high-gain multibeam ambient RF energy harvesting system utilizing hybrid combining. *IEEE Transactions on Industrial Electronics*, 67(11), 9215-9226.
- [29]. Alam, S., Surjati, I., Ningsih, Y. K., Sari, L., Syukriati, E., & Safitri, A. (2019, October). Design of Truncated Microstrip Antenna with Array 4×2 for Microwave Radio Communication. In *2019 IEEE Conference on Antenna Measurements & Applications (CAMA)*, 1-4. IEEE.
- [30]. Zou, Y., Li, H., Xue, Y., & Sun, B. (2019). A high-gain compact circularly polarized microstrip array antenna with simplified feed network. *International Journal of RF and Microwave Computer-Aided Engineering*, 29(12), e21964.
- [31]. Du, Z. X., Bo, S. F., Cao, Y. F., Ou, J. H., & Zhang, X. Y. (2020). Broadband circularly polarized rectenna with wide dynamic-power-range for efficient wireless power transfer. *IEEE Access*, 8, 80561-80571.
- [32]. Fakharian, M. M. (2020). A wideband rectenna using high gain fractal planar monopole antenna array for rf energy scavenging. *International Journal of Antennas and Propagation*, 2020, 1-10.

- [33]. Sun, W., Li, Y., Chang, L., Li, H., Qin, X., & Wang, H. (2021). Dual-band dual-polarized microstrip antenna array using double-layer gridded patches for 5G millimeter-wave applications. *IEEE Transactions on Antennas and Propagation*, 69(10), 6489-6499.
- [34]. Khan, J., Ullah, S., Ali, U., Tahir, F. A., Peter, I., & Matekovits, L. (2022). Design of a millimeter-wave MIMO antenna array for 5G communication terminals. *Sensors*, 22(7), 2768.
- [35]. Kim, S., Yoon, S., Lee, Y., & Shin, H. (2019). A miniaturized Butler matrix based switched beamforming antenna system in a two-layer hybrid stackup substrate for 5G applications. *Electronics*, 8(11), 1232.
- [36]. Trinh-Van, S., Lee, J. M., Yang, Y., Lee, K. Y., & Hwang, K. C. (2019). A Sidelobe-Reduced, Four-Beam Array Antenna Fed by a Modified 4×4 Butler Matrix for 5G Applications. *IEEE Transactions on Antennas and Propagation*, 67(7), 4528-4536.
- [37]. Lee, S., Lee, Y., & Shin, H. (2021). A 28-GHz switched-beam antenna with integrated Butler matrix and switch for 5G applications. *Sensors*, 21(15), 5128.
- [38]. Ashraf, N., Sebak, A. R., & Kishk, A. A. (2020). PMC packaged single-substrate 4×4 Butler matrix and double-ridge gap waveguide horn antenna array for multibeam applications. *IEEE Transactions on Microwave Theory and Techniques*, 69(1), 248-261.